Environment, Development and Sustainability
https://doi.org/10.1007/s10668-025-06072-z

Effectiveness of urban parks in reducing ambient PM_{10} through deposition and dispersion: towards greener cities

Mohammad Moftakhar Juybari[1] · Seyed Mahdi Heshmatol Vaezin[1] · Mazaher Moeinaddini[5] · Satoshi Hirabayashi[2] · Anoshirvan Shirvany[1] · Reza Shahbazi[3] · Nahid Ahmadi[3] · Seyed Mohammad Moein Sadeghi[4]

Received: 9 May 2024 / Accepted: 19 February 2025
© The Author(s), under exclusive licence to Springer Nature B.V. 2025

Abstract
As the 'lungs of the city' and a refuge from pollutants, urban parks improve air quality by reducing ambient PM_{10} through deposition and dispersion, particularly in major metropolises. This study evaluates the average relative reduction effect of urban parks on ambient PM_{10}at the respiratory level (1.5 -2 m above ground) through deposition and dispersion, focusing on two widely planted tree species across the Middle East—oriental plane (*Platanus orientalis* L.) and white mulberry (*Morus alba* L.)—. These species are commonly used in urban green spaces due to their adaptability, broad canopy, and ability to withstand urban stressors. The research was conducted in Laleh Park, located in the heart of Tehran, one of the most polluted cities in the world. We developed a combined procedure integrating theoretical model (i.e., dry deposition flux) with both direct and indirect measurements of ambient PM_{10}. We applied a dry deposition flux model using locally derived, seasonally adjusted deposition velocities for PM_{10} and $PM_{2.5}$ on tree leaves, estimated through indirect measurements. Then, direct measurements taken inside and outside Laleh Park were used to disaggregate the park's effectiveness on ambient PM_{10} into deposition and dispersion effects. The theoretical model showed that the park's trees contributed to a 10% total reduction in ambient PM_{10} at the respiratory level through deposition over the course of a year, with oriental plane trees accounting for a 9.3% reduction and white mulberry trees contributing an additional 0.7%. Direct measurements confirmed this finding, showing that the park's trees contributed to an average 10.4% reduction in ambient PM_{10} at the respiratory level through deposition over year. Furthermore, the dispersion of PM_{10} within the park accounted for an average 6.1% reduction in ambient PM_{10}. Altogether, the combined effect of deposition and dispersion led to an average 16.5% reduction in ambient PM_{10} at the respiratory level inside the park. Elemental analysis of foliar deposits revealed elevated concentrations of Al and Pb, with enrichment factors of 110 and 7, respectively. The extremely high enrichment of Al and significant enrichment of Pb indicate strong anthropogenic contributions, likely from traffic-related sources. These findings highlight the potential for urban parks in cities like Tehran, to improve air quality, with implications for more effective urban planning. Further research is needed to assess the broader effectiveness of various types of urban green spaces (e.g., urban forests, parks, community gardens, and greenways) and plant species in mitigating different types of pollutants.

Extended author information available on the last page of the article

Published online: 17 April 2025

Content courtesy of Springer Nature, terms of use apply. Rights reserved.

Keywords Dispersion · Dry deposition flux · Direct PM_{10} measurement · Air quality improvement · PM size distribution · PM elemental composition · Leaf washing

1 Introduction

Air pollution is responsible for approximately 4.2 million premature deaths worldwide every year (WHO, 2021). Among the various pollutants, particulate matter (PM) poses one of the most serious health risks in urban environments, particularly in large metropolitan areas, as it is linked to a wide range of respiratory and cardiovascular diseases (Beckett et al., 1998). PM with a diameter of 10 µm or less (PM_{10}) and 2.5 µm or less ($PM_{2.5}$) are especially harmful, as smaller particles can penetrate deeper into respiratory system, increasing health risks (Beckett et al., 1998; Xing & Sun, 2019). In addition, $PM_{2.5}$ often contains toxic heavy metals such as chromium (Cr), cadmium (Cd), arsenic (As), lead (Pb), and nickel (Ni), which can be dangerous even at low concentrations. In 2018, the European Environment Agency (EEA) found that $PM_{2.5}$ exposure contributed to approximately 417,000 annual premature deaths in 41 European countries (Sanchez-Pinero et al., 2022). Finally, PM_{10} is especially problematic in urban areas due to high traffic and reduced wind speeds, which lead to high concentrations of these particles.

According to the World Health Organization (WHO) factsheet on policies to reduce air pollution, maintaining and expanding urban tree cover is crucial for achieving this purpose, complementing efforts to control traffic-related pollution (WHO, 2021). As the 'lungs of the city' and a refuge from pollutants, urban parks provide a cost-effective strategy for improving and monitoring air quality (Beckett et al., 1998; Escobedo et al., 2008; Hirabayashi, 2014; Rasoolzadeh et al., 2024a). Urban parks act as natural Air Handling Units (AHU) or urban biofilters, where airborne particles deposit on a multi-layered vegetation. Studies have shown that approximately 59.7% of the total suspended particulate (TSP) deposited on the leaves of the oriental plane (*Platanus orientalis* L.) trees in Tehran (Heshmatol Vaezin et al., 2021), and 73% in various European cities (Baldacchini et al., 2017), consist of PM_{10}. In addition to dry deposition, urban parks contribute to the reduction of ambient PM_{10} through dispersion (Janhäll, 2015; Morakinyo & Lam, 2016; Xing & Brimblecombe, 2019). Dispersion refers to the transport, spreading, and dilution of pollutants in the ambient air as moving away from the source (horizontally and vertically) due to atmospheric factors (e.g., wind, and turbulence). In open spaces and parks, dispersion may be enhanced by interaction of air flow with urban trees (Xing & Brimblecombe, 2019) through mechanical turbulence and thermal uplift, or by guiding airflow at a larger scale. Nevertheless, dense urban tree canopies may reduce dispersion by restricting airflow (Xing & Brimblecombe, 2019). In urban parks, trees contribute to reducing ambient PM_{10}through dry deposition, where particles settle on leaves, trunks, and branches (Heist et al., 2013; Janhäll, 2015). In addition, ambient PM_{10} disperses within urban parks.The relative reduction effect of urban trees on ambient PM_{10} through dry deposition has often been quantified using the framework developed by Nowak and Crane (1998). We also applied this franework to quantify the dispersion of PM_{10} within the park. Generally, empirical and theoretical approaches have been employed to estimate the reduction effect of urban parks on ambient PM_{10} through deposition and dispersion processes (Heshmatol Vaezin et al., 2021; Tallis et al., 2011; Xing & Brimblecombe, 2019; Xing & Brimblecombe, 2019). In the first approach, this effect is inferred either

Content courtesy of Springer Nature, terms of use apply. Rights reserved.

directly, by measuring ambient PM_{10} (e.g., with measuring instruments; TSI device), or indirectly, through quantifying PM_{10} deposition on tree leaves (e.g. by leaf washing or using Scanning Electron Microscopy) (Vigevani et al., 2024). Direct measurements serve to estimate the effect of deposition and dispersion in urban parks (Xing & Brimblecombe, 2019). Nevertheless, they have limitations, such as high variability in time and space, leading to high sampling costs, particularly in the absence of monitoring stations. Based on theoretical models like dry deposition flux model, the second approach is less costly to apply (Tallis et al., 2011; Xing & Brimblecombe, 2019) but estimates the effect of urban parks on ambient PM_{10} only through deposition process (Xing & Brimblecombe, 2019). This method is often applied based on an average deposition velocity of 0.0064 m s^{-1} for a reference LAI (Leaf Area Index) of 6 (m^2 m^{-2}) (Escobedo & Nowak, 2009; Hirabayashi, 2014; Pace, 2019). Yet, deposition velocity is highly variable as it depends on species (including leaf area index), vegetation structure (Beckett et al., 1998), particle size, ambient PM_{10} (Beckett et al., 1998; Sohrab et al., 2022) and wind speed (Pröhl et al., 2012; Beckett et al., 1998), among other factors. Many studies have quantified the relative reduction effect of PM_{10} by urban trees using theoretical models on a large scale (e.g., city-wide) (Escobedo & Nowak, 2009; Hirabayashi et al., 2012; Nowak et al., 2014; Tallis et al., 2011). This approach was also applied by computer software tools such as i-Tree Eco and i-Tree Streets (Hirabayashi et al., 2012; Nowak & Crane, 1998). However, the results of theoretical models are poorly supported by empirical evidence (Yin et al., 2011; Abbaspour et al., 2014; Xing & Brimblecombe, 2019), especially at local level (e.g., an urban park).

This research aims to provide empirical evidence on the average relative reduction effect of urban parks on ambient PM_{10} at the respiratory level through deposition and dispersion processes over the course of a year. To achieve this, we developed a combined theoretical and empirical procedure. The research was conducted in Laleh Park, located in the heart of Tehran, one of the most polluted cities in the world. The contribution of this study is threefold. First, a dry deposition flux model (Chamberlain, 1953; Lovett, 1994; Nowak & Crane, 1998; Freer-Smith et al., 2005; Heshmatol Vaezin et al., 2021) was applied at the respiratory level, to better assess human exposure (i.e., pedestrian level, 1.5–2 m above ground; Yin et al., 2011; Xing & Brimblecombe, 2019; Heshmatol Vaezin et al., 2021). Second, indirect measurements were used to calibrate the theoretical model (via deposition velocity), scale up deposition estimates (from tree to park scale), and extrapolated them from the spring–summer period to an annual scale (Heshmatol Vaezin et al., 2021). Unlike Heshmatol Vaezin et al (2021), which estimated deposition velocity for TSP, this study separately estimates it for PM_{10} and $PM_{2.5}$. We estimated a locally derived, seasonally adjusted deposition velocity on tree leaves using the leaf washing technique (Heshmatol Vaezin et al., 2021). Moreover, direct measurements of PM_{10} (Abbaspour et al., 2014) were used to benchmark the calibrated model's estimate at the park scale and disaggregate the park's effectiveness on ambient PM_{10} into deposition and dispersion (Yin et al., 2011; Xing & Brimblecombe, 2019). Third, this study further explores the size distribution, elemental composition, and enrichment factor of foliar deposits, providing a more detailed understanding of particulate matter captured by urban trees. By highlighting the role of urban parks in dispersing and depositing airborne PM, urban planners and environmental managers can better recognize and enhance the ecological services these green spaces provide, contributing to greener and healthier cities.

Content courtesy of Springer Nature, terms of use apply. Rights reserved.

2 Materials and methods

2.1 Study site

Tehran, the capital of Iran and the largest city in the Middle East, is a rapidly growing metropolis facing major environmental challenges, particularly health issues linked to particulate air pollution (Rasoolzadeh et al., 2024a, b). This study was conducted in the 6th district of Tehran municipality, located near city center, an area with the heaviest traffic (Municipality of Tehran, 2023). Laleh Park (35°42'N; 51°23'E; elevation: 1231–1253 m asl), situated in the heart of this district, was chosen as the study site due to its extensive green space, covering 28 ha (equivalent of a 529 m × 529 m square). The park is bordered by high-traffic streets on all sides, making it an ideal location to study the impact of urban parks on air quality. The two dominant tree species in Tehran (Municipality of Tehran, 2023), oriental plane (*Platanus orientalis* L.; Taxonomic Serial Number: 19436) and white mulberry (*Morus alba* L.; Taxonomic Serial Number: 501831), were selected for this study. Both species are well-known for their drought tolerance and pest resistance, making them popular choices in Tehran's green spaces and other semiarid regions. Additionally, these species are extensively planted across the Middle East, where they play a crucial role in urban greening, dust mitigation, and environmental resilience in water-scarce landscapes.

At the study site, the primary sources of TSP are traffic-related emissions. Measurements taken around the park's perimeter indicate that the annual mean concentrations of local PM_{10} at the respiratory level was 113.8 μg m^{-3} (Abbaspour et al., 2014), which is 7.6 times higher than the WHO air quality guideline for PM_{10} (15 μg m^{-3}) in 2021 (WHO, 2021). Moreover, the climatic data for the study site includes a mean annual temperature of 16.5 °C, and average wind speed of 1.5 m s^{-1}.

2.2 Sampling

Sample trees were selected using linear systematic random sampling along several randomly placed transects throughout the park in late summer 2020. The number of sample trees and leaves per sample tree in the study area was determined using Cochran's formula at a 95% confidence interval (Cochran, 2012). Following the sampling procedure outlined by Heshmatol Vaezin et al. (2021) and (Song et al., 2015), the first sample tree was randomly selected, and subsequent trees were selected with an inter-tree distance of approximately 100 m (Fig. 1). As a result, 53 sample trees were selected (oriental plane = 30 trees and white mulberry = 23 trees). For leaf sampling, 63 leaves per oriental plane tree and 50 leaves per white mulberry were randomly collected from each cardinal direction at a height of 2 m using scissors. For further details on data collection, please refer to Heshmatol Vaezin et al. (2021).

2.3 Estimation procedure

We combined both empirical (2.3.1) and theoretical (2.3.2) approaches to estimate the average relative reduction effect of urban parks on ambient PM_{10} at the respiratory level through deposition and dispersion processes over the course of a year. The combined empirical and theoretical procedure (2.3.3) is illustrated through a flowchart in Fig.2.

The average relative reduction of PM_{10} within urban parks (AQI%) (Nowak & Crane, 1998; Xing & Brimblecombe, 2019), is also referred to as air quality improvement rate.

Content courtesy of Springer Nature, terms of use apply. Rights reserved.



Fig. 1 Location of sample trees in Laleh Park. Green points represent white mulberry trees, and yellow points represent oriental plane trees

This was calculated based on the total grams of PM_{10} removed each year (GR) relative to the total grams of PM_{10} present in the atmosphere (GA + GR; Nowak & Crane, 1998) (Eq. 1):

$$AQI\% = \frac{GR}{(GA + GR)} \times 100 \tag{1}$$

where AQI% represents the percentage improvement in air quality, while GR is the grams of PM_{10} removed annually either through deposition on vegetation or through dispersion at the respiratory level, and GA (g) is the grams of PM_{10} present in the atmosphere over the year (Nowak & Crane, 1998; Nowak and Crane 2006). GR was estimated empirically using both direct (2.3.1.1) and indirect (2.3.1.2) measurements, while GA was calculated according to Eq. 2:

$$GA = C(H) \times H \times A \tag{2}$$

In this equation, C(H) is the mean annual concentrations of local PM_{10} at respiratory height (H), and A is the contact area (i.e., the region covered or affected by urban parks). The mean annual concentrations of local PM_{10} at the respiratory level (H) was considered as 113.8 μg m^{-3} (Abbaspour et al., 2014). This PM_{10} concentration at H level was used in Eq. 2 to calculate the total grams of PM_{10} present in the atmosphere. The exact area of the park was calculated using the polygon area measurement tool in Google Maps.

2.3.1 Empirical approach

The empirical approach assess the average relative reduction of PM_{10} at the respiratory level inside urban parks either directly, by measuring ambient PM_{10} using monitoring instruments (e.g., TSI device), or indirectly, through quantifying PM_{10} deposition on

Content courtesy of Springer Nature, terms of use apply. Rights reserved.

park trees (e.g., gravimetric analysis of foliar deposits, also known as the leaf washing technique).

2.3.1.1 Direct measurements Direct measurements of ambient PM_{10} were used to approximate the average relative reduction of ambient PM_{10} at the respiratory level inside urban parks through deposition and dispersion processes (Xing & Brimblecombe, 2019). Abbaspour et al. (2014) established a network of monitoring stations (as shown in Fig. 3) to measure PM_{10} levels both within Laleh Park (within 200 m of the park boundaries) along its borders, and in the surrounding residential areas. As depicted in Fig. 3, the monitoring network consisted of 16 stations, strategically distributed to capture spatial gradients of PM_{10} concentrations. Stations 2 and 3 were located at the core of the park, while stations 1, 4, 5, 7, 8, 9, 10, 11and 15 were positioned along the park perimeter (Fig. 3). Measurements were conducted monthly, during both morning and evening hours, from summer 2010 to spring 2011, using a TSI Dust Tracker (Model 8520, Shoreview, MN, USA) at the respiratory level (H).

Figure 3 highlights the spatial pattern of PM_{10} reduction both inside and outside the park, revealing a clear gradient aligned with the local wind direction (northeast to southwest). Across the park, this pattern shows a distinct PM_{10} gradient, decreasing from the borders toward the core. The gradient is observed along downwind diagonal transects (northeast to southwest), which extend from the park's borders toward its innermost areas throughout the park. These transects vary in length, averaging approximately 200 meters. The data from the measurement stations (Abbaspour et al., 2014) revealed a distinct negative gradient in annual mean PM_{10} concentrations along a 200-m downwind transect inside the park, from the borders toward the park's core. The percentage change in ambient PM_{10} along this gradient represents the average effect of deposition and dispersion within the park (Xing & Brimblecombe, 2019). Using data from measurement stations and PM_{10} gradient maps (Abbaspour et al., 2014), a similar negative gradient was observed along 200-m downwind transects in residential areas bordering the park on all four sides (North, East, South, and West). The percentage change in ambient PM_{10} along this gradient was assumed to represent the average dispersion effect inside and outside the park. The effectiveness of the park's trees on ambient PM_{10} was then estimated by comparing the percentage change in PM_{10} along 200-m downwind transects under two scenarios: (1) with trees (inside the park, factual situation) and (2) without trees (outside the park, counterfactual situation; Heshmatol Vaezin et al., 2021). The total grams of PM_{10} deposited on park trees (bark and leaves) or reduced through dispersion over the year (GR) was calculated by multiplying the corresponding percent change by the mean annual concentrations of PM_{10} at the respiratory height (C(H)) and the park area. Then, the average relative reduction effect of the park's trees on ambient PM_{10} was quantified using Eq. 1. Similarly, the average relative reduction effect due to PM_{10} dispersion within the park was also approximated. As such, direct measurements allowed us to disaggregate the park's combined effect on ambient PM_{10} into deposition and dispersion.

2.3.1.2 Indirect measurements Measuring foliar deposits and estimating total leaf area were incorporated into the indirect measurements of PM_{10}, as they contribute to assessing foliar PM_{10} deposition. Moreover, we analyzed foliar deposits for particle size distribution, elemental composition, and enrichment factors to gain deeper insights into particulate matter captured by urban trees. The leaf washing technique was used to estimate foliar PM_{10} deposits per unit leaf area over time (deposition flux, F; $gm^{-2}\ s^{-1}$), as

Content courtesy of Springer Nature, terms of use apply. Rights reserved.

well as the total amount of foliar PM_{10} deposition per tree during spring and summer. The sample leaves collected from the sample trees were washed with 150 ml of distilled water and 15 ml of chloroform solution, using a soft brush to remove remaining TSP, including traffic-related black carbon, from the epicuticular waxes (Sgrigna et al., 2015). For more details on the centrifugation, drying and, weighing of the samples, refer to Heshmatol Vaezin et al. (2021). The size distribution of foliar deposits, along with the volume percentage of PM_{10} and $PM_{2.5}$, were determined using the Fritsch Analysette 22 (Fritsch GmbH, Idar-Oberstein, Germany) (Memoli et al., 2020). To obtain the weight percentage of PM_{10} and $PM_{2.5}$, the dry volume of the samples was measured with a 5 ml graduated cylinder and weighted using a high precision laboratory balance (A&D GF-1000, USA, with a 0.0001 g accuracy). The TSP sample was mixed with a spatula, after which a random portion was taken and weighed. The sample was then dissolved in deionized water, placed in the Fritsch Analysette 22, and the volume percentage of TSP was reported, covering particle sizes ranging from < 0.1 µm to approximately 50 µm (Fig. 4). Then, the volume percentage was converted to the weight percentage of TSP using the bulk density formula (Eq. 3; Dadey et al., 1992).

$$DBD = \frac{W}{V} \tag{3}$$

DBD represents the dry bulk density of the samples (g ml^{-1}), where W denotes the weight of the dry sample (g), and V corresponds to the dry sample volume (ml). The weight percentage of PM_{10} in foliar deposits was then calculated by multiplying DBD by the volume percentage of PM_{10}. As a result, the average foliar deposition of PM_{10} per sample leaf or per unit leaf area was calculated for both spring and summer.

The leaf area index (LAI; m^2 m^{-2}) was derived from photographs of tree crowns using a fisheye camera, Canon EOS 6D (Tokyo, Japan) (Deljouei et al., 2018; Heshmatol Vaezin et al., 2021; Sadeghi et al., 2017). Subsequently, the canopy cover area (CCA; m^2), total leaf area (TLA; m^2), and leaf number (N) of each sample tree were estimated (Appendix A; Blanco & Folegatti, 2003). Consequently, the total amount of foliar PM_{10} deposition per tree during spring and summer was obtained by multiplying the leaf number of each sample tree by the average PM_{10} deposition per leaf (Heshmatol Vaezin et al., 2021; Song et al., 2015).

Three samples of foliar deposits were sieved through a 63 µm sieve, homogenized, and, chemically analyzed (Mihankhah et al., 2020). For the analysis, 0.1 g and 0.5 g of each dust sample were digested with 10 ml of aqua regia ($HCl:HNO_3 = 3:1$) at 80 °C for 2 hours. After digestion, the solution was concentrated to 100 ml and 50 ml for Inductively Coupled Plasma Mass Spectrometry (ICP-MS) and Inductively Coupled Plasma Optical Emission Spectroscopy (ICP-OES) analysis, respectively. Then, the solutions underwent were analyzed for 16 elements (Al, Ca, Cd, Co, Cr, Cu, Fe, K, Mg, Mn, Mo, Na, Ni, Pb, V, and Zn) using an ICP-MS (Perkin Elmer Elan Sciex 9000) device at the Iranian Geological Survey and Mineral Exploration. The enrichment factor (EF) formula (Eq. 4) was utilized to assess heavy metal contamination levels and to distinguish between natural and anthropogenic sources (Sakunkoo et al., 2022; Zoller et al., 1974).

$$EF = \frac{\left(\frac{MCD}{RE}\right)_{in\ deposition}}{\left(\frac{MCB}{RE}\right)_{in\ background}} \tag{4}$$

Content courtesy of Springer Nature, terms of use apply. Rights reserved.

where RE is the concentration of the reference element, a geogenic metal (mg kg^{-1}). Additionally, MCD and MCB represent the concentration of the metal in foliar deposits and the background level for Iran (mg kg^{-1}), respectively. An EF value close to 1 indicates no significant enrichment, suggesting that the element predominantly originates from natural crustal sources.

2.3.2 Theoretical approach

In the absence of precipitation, dry deposition flux (F; μg m^{-2} s^{-1}) is a theoretical model (Chamberlain, 1953; Lovett, 1994) that can provide a cost-effective alternative to field measurements. This model has been widely used in the Urban Forest Effects model (UFORE: Nowak & Crane, 1998) and i-Tree Eco software (Hirabayashi et al., 2012), as well as in numerous studies evaluating the role of urban trees in reducing ambient PM_{10} levels (Nowak & Crane, 1998; Rasoolzadeh et al., 2024b; Tallis et al., 2011).

PM_{10} deposited ($PM_{10}D$; μg) on tree leaves and bark (including trunks and branches) results from the collision between instantaneous dry deposition flux of PM_{10} (F; μg m^{-2} s^{-1}) and the tree's contact area over a specified time (Heshmatol Vaezin et al., 2021; Nowak & Crane, 1998). $PM_{10}D$ was estimated by multiplying the instantaneous dry deposition flux per unit areas (F; gm^{-2} s^{-1}), the contact area (A; m^2), and the contact time (T; s), as follows (Eq. 5):

$$PM_{10}D = F \times A \times T \tag{5}$$

$$F = VD \times C(H) \tag{6}$$

where VD is the deposition velocity for PM_{10} (m s^{-1}), and C(H) is the mean concentrations of local PM_{10} (μg m^{-3}) during the contact time (T).

2.3.3 Estimation procedure

A combined estimation procedure (Fig. 2) was developped based on empirical (Section 2.3.1) and theoretical (Section 2.3.2) approaches. Similar to tree leaves, tree bark (including trunk and branches) is also exposed to ambient PM_{10}; however, we did not have measurements of PM_{10} deposits on the bark. Moreover, since most precipitation falls in autumn and winter in Tehran (Sadeghi et al., 2017), and leaf fall takes place during winter, applying the leaf wash technique is not feasible for these seasons. As a result, a combined estimation procedure was used to estimate the yearly whole-tree PM_{10} deposition (Fig. 2). In general, the combined procedure was used to empirically calibrate the theoretical model (via deposition velocity), scale up deposition estimates (from tree leaves to whole-tree and park scales), and extrapolate them from the spring–summer period to an annual scale through indirect measurements. Finally, direct measurements were used to benchmark the deposition estimate at the park level and to disaggregate the park's effectiveness on ambient PM_{10} into deposition and dispersion effects.

Using a locally estimated deposition velocity for PM_{10}, a dry deposition flux model was applied to approximate the yearly whole-tree PM_{10} deposition. We estimated the site- and species-specific dry deposition velocity (VD), based on the quotient between the PM_{10} deposition flux (Eq. 6) measured on tree leaves (μg m^{-2} s^{-1}) and the local mean of PM_{10} concentrations during spring and summer (Heshmatol Vaezin et al.,

Content courtesy of Springer Nature, terms of use apply. Rights reserved.

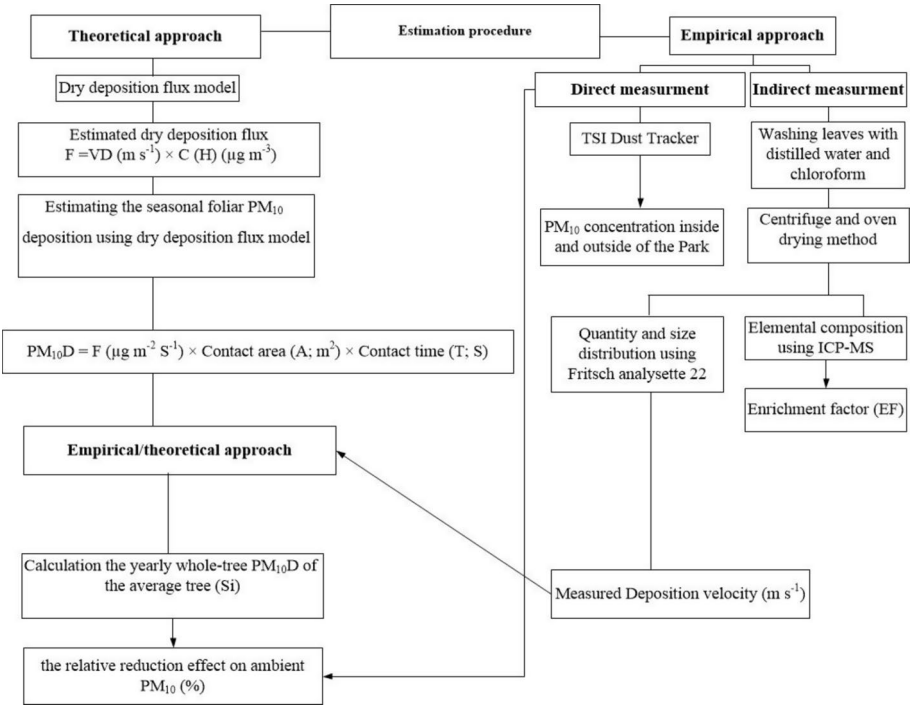


Fig. 2 Estimation procedure used to estimate the average relative reduction of ambient PM_{10} in urban parks through deposition and dispersion

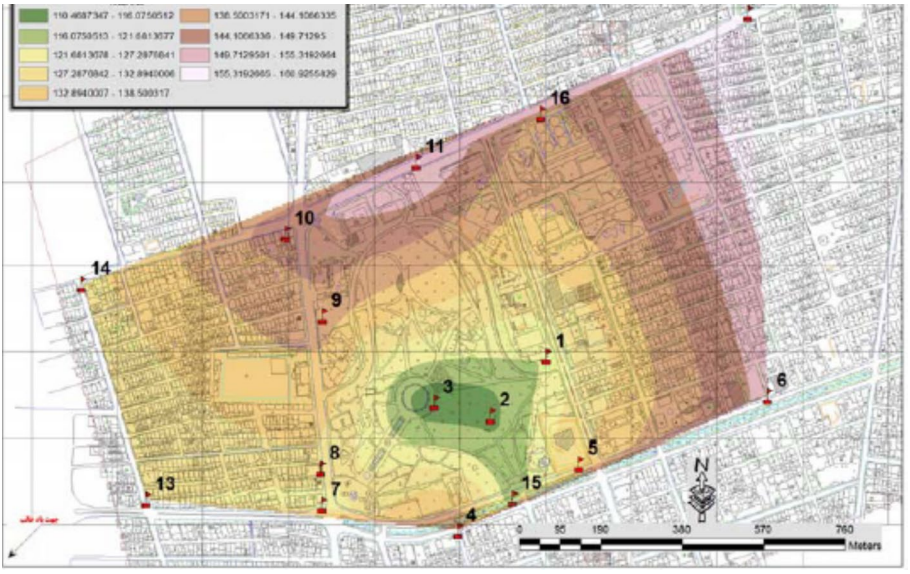


Fig. 3 Locations of PM_{10} monitoring stations (1–14) inside (200 m from park boundaries) and outside Laleh Park, and PM_{10} gradient Map for winter (adopted from Abbaspour et al., 2014)

Content courtesy of Springer Nature, terms of use apply. Rights reserved.

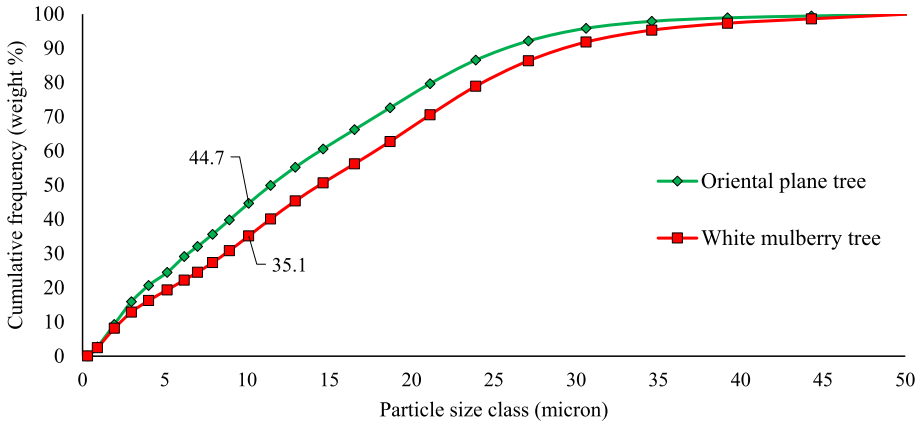


Fig. 4 Particle size distribution of foliar deposits in Laleh Park, Tehran

2021). The dry deposition velocity estimated for spring and summer was then adjusted for autumn and winter based on seasonal variations in leaf area index (LAI; Hirabayashi et al. 2015; Appendix B). Next, the bark area index (BAI; $m^2\ m^{-2}$) was calculated as the sum of trunk and branch area indices according to the procedure developed by Heshmatol Vaezin et al. (2021). The plant area index (PAI; m^2m^{-2}) was obtained from the sum of BAI and LAI. Finally, the total plant area was calculated by the product of PAI and the CCA. Seasonal dry deposition velocities and the total plant area were then employed to calculate whole-tree PM_{10} deposition of the sample tree i (S_i) in each season (Appendix B). Then, the yearly whole-tree PM_{10} deposition of the sample tree i was calculated by summing the seasonal whole-tree PM_{10} depositions over the year. Finally, we calculated the yearly whole-tree PM_{10} deposition for the average tree as follows (Eq. 7):

$$WS = \frac{\sum_{i=1}^{n} S_i DBH_i^{\ 2}}{\sum_{i=1}^{n} DBH_i^2} \tag{7}$$

where WS is the yearly whole-tree PM_{10} deposition of the average tree, and S_i and DBH_i were the yearly whole-tree PM_{10} deposition and the DBH of the sample tree *i*, respectively. The annual PM_{10} deposition of the average tree was then generalized to Laleh Park and Tehran's 6th district based on the total number of oriental plane and white mulberry trees recorded in the park and the 6th municipality district (Municipality of Tehran, 2023). Finally, the average reduction effect of park trees on ambient PM_{10} (Eq. 1) was calculated based on yearly whole-tree PM_{10} estimate at the park level.

2.4 Statistical test

The comparison of the two tree species in terms of the weight percentage of PM_{10} in foliar deposits was conducted using a paired t-test in SPSS software (Version 24). This test was chosen to determine whether the mean PM_{10} deposition differed significantly between the two species. Before performing the analysis, the data were assessed for

Content courtesy of Springer Nature, terms of use apply. Rights reserved.

normality using the Shapiro–Wilk test to ensure the paired t-test assumptions were met. The null hypothesis posited no significant difference in PM_{10} deposition between the species. Descriptive statistics, including the mean, standard deviation, and 95% confidence intervals, were calculated for each species to contextualize the analysis. The paired t-test provided key outputs, such as the t-statistic, degrees of freedom, and p-value, which were used to determine the significance of the observed differences.

3 Results

3.1 Samples descriptions

The descriptive statistics for the 53 sample trees (30 oriental plane and 23 white mulberry trees) are presented in Table 1. The results show that the average (±SE) DBH for oriental plane trees was 40.1 cm (±5.9 cm), while for white mulberry trees, it was 22.6 cm (±3.4 cm). Additionally, the average canopy cover area for oriental plane trees was 4.87 m^2 (±0.91 m^2), compared to 1.87 m^2 (±0.31 m^2) for white mulberry trees (Table 1).

3.2 Foliar deposits analysis (quantity, size distribution and elemental composition)

Foliar deposits from spring to summer were measured at 0.33 mg cm^{-2} (±0.05) for oriental plane and 0.31 mg cm^{-2} (±0.09) for white mulberry. In contrast, the average $PM_{2.5}$ and PM_{10} deposition on the leaves of oriental plane tree during spring and summer (six-month period) were 0.044 mg cm^{-2} (±0.013) and 0.17 mg cm^{-2} (±0.04), respectively. Similarly, the average $PM_{2.5}$ and PM_{10} deposition on the leaves of white mulberry tree were 0.025 mg cm^{-2} (±0.01) and 0.12 mg cm^{-2} (±0.03), respectively. The foliar PM_{10} deposits across the park showed a negative gradient, with an average reduction effect of 16.5% (Fig. 5) along a 200-m downwind transect from the eastern boundary into the park's core.

The weight percentage of PM_{10} in the foliar deposits of oriental plane and white mulberry leaves averaged 44.7% and 35.1% respectively (Table 2 and Fig. 4). The result of

Table 1 Descriptive statistics of the morphological characteristics of sample trees in Laleh Park

Morphological characteristics	Oriental plane			White mulberry		
	Mean	Max	Min	Mean	Max	Min
Diameter at breast height (DBH) (cm)	40.07	51.70	30.50	22.62	28.50	17.50
Tree height (m)	9.19	11.39	7.00	3.05	4.35	2.10
Canopy cover area (CCA) (m^2)	4.87	7.10	3.09	1.87	2.52	1.31
Single-sided leaf area (cm^2)	116.83	291.44	40.03	105.51	187.59	48.04
Number of leaves (N)	1070	1288	841	503	735	365
Total leaf area (TLA) (m^2)	12.40	18.40	18.28	5.51	8.03	3.97
Leaf area index (m^2 m^{-2})	2.17	2.99	1.45	2.15	3.32	0.75
Branch area index (m^2 m^{-2})	0.14	0.21	0.10	0.08	0.13	0.04
Trunk area index (m^2 m^{-2})	1.49	2.22	0.64	0.06	0.12	0.04
Plant area index (m^2 m^{-2})	3.23	5.17	0.75	3.30	2.59	1.87

Content courtesy of Springer Nature, terms of use apply. Rights reserved.

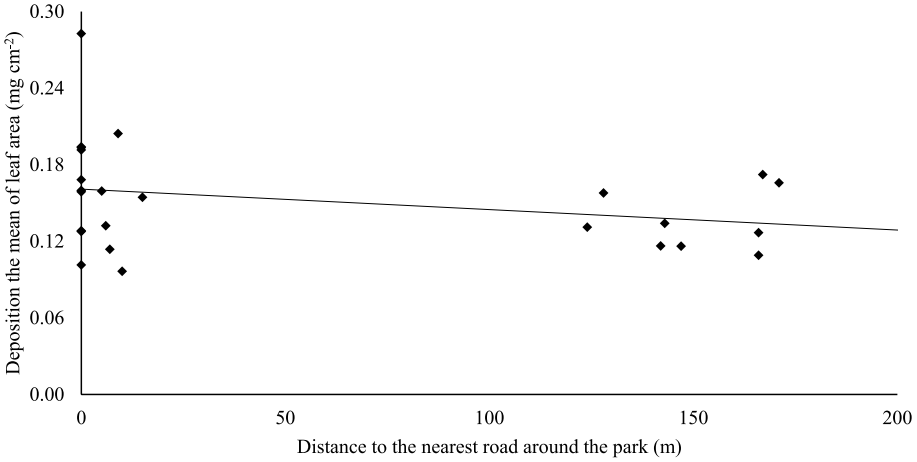


Fig. 5 Downwind gradient of foliar PM_{10} deposition on oriental plane trees in Laleh Park during the spring–summer period

Table 2 The comparison of the mean weight percentage of PM_{10} deposited on oriental plane and white mulberry trees in Laleh Park

Species	Weight % PM_{10}	t-student	d_f	Mean different	St. Err. mean	CL 95%	
						Lower	Upper
Oriental plane	44.7	7.46	23	5.67	0.76	4.10	7.24
White mulberry	35.1						

the paired t-test confirms that the two species differ significantly in their PM_{10} deposition (Table 2). Specifically, oriental plane trees deposited 27.4% more PM_{10} than white mulberry trees, all else being equal (Table 2).

The results of the ICP-MS analysis revealed the following increasing order of elemental concentrations in foliar deposits (mg kg^{-1}): Zn = 779 > Mn = 770 > Cu = 240 > Pb = 119 > Cr = 101 > Ni = 44 > Co = 13 > Al = 6 (Table 3). Among these, zinc (Zn) had the highest mean concentration at 779 mg kg^{-1} (Table 3). However, the aluminum (Al) exhibited the highest enrichment factor (EF = 110), indicating as extremely high level of enrichment.

3.3 Deposition velocity

The average foliar deposition velocity for $PM_{2.5}$ and PM_{10} on oriental plane trees during the spring–summer period was calculated to be 0.0011 m s^{-1} (± 0.00) and 0.0017 m s^{-1} (± 0.001), respectively. Yearly whole-tree PM_{10} deposition of oriental plane and white mulberry trees were estimated to be in average 52.0 g and 15.9 g, respectively (Fig. 6).

Content courtesy of Springer Nature, terms of use apply. Rights reserved.

Table 3 Descriptive statistics of elemental composition in foliar deposits from three foliar dust samples of oriental plane trees. Due to financial limitations, no attempt was made to analyze heavy metals in white mulberry trees.

Elements	Mean (mg kg^{-1})	St Dev (±)	Min	Max	Enrichment Factor (EF)	EF degree
Al	6.43	0.28	6.20	6.75	110	EF > 40 (extremely high enrichment)
Ca	8.13	0.22	7.87	8.26	0.5	EF < 2 (depletion to mineral enrichment)
Cd	0.61	0.35	0.27	0.96	2	2 ≤ EF < 5 (moderate enrichment)
Co	13.4	0.94	12.4	14	1	EF < 2 (depletion to mineral enrichment)
Cr	101	3.05	98	104	1	EF < 2 (depletion to mineral enrichment)
Cu	240	3.61	235	245	8.8	5 ≤ EF < 20 (significant enrichment)
Fe	4.17	0.11	4.04	4.26	1	EF < 2 (depletion to mineral enrichment)
K	1.58	0.11	1.46	1.66	1	EF < 2 (depletion to mineral enrichment)
Mg	1.86	0.04	1.82	1.91	0.5	EF < 2 (depletion to mineral enrichment)
Mn	770	39.71	724	794	1	EF < 2 (depletion to mineral enrichment)
Na	1.11	0.06	1.06	1.18	0.4	EF < 2 (depletion to mineral enrichment)
Ni	44	2.80	40	45	0.4	EF < 2 (depletion to mineral enrichment)
Pb	119	15.29	101	129	6.6	5 ≤ EF < 20 (significant enrichment)
V	77	4.80	72	80	–	–
Zn	779	8.07	770	789	–	–

3.4 Relative reduction effect

Direct measurements of ambient PM_{10} showed an average relative reduction effect of 16.5% at the respiratory level inside the park over the course of the year. Additionally, these measurements revealed an average 10.4% relative reduction of PM_{10} at the respiratory level inside the park, attributed to park vegetation throughout the year. Direct measurements also revealed an average 6.1% relative reduction effect due to the dispersion of PM_{10} within the park. Similarly, indirect measurements confirmed an average reduction effect of 10% at the respiratory respiratory level of the park, with 9.3% attributed to oriental plane and 0.7% to white mulberry trees over the study year (Table 4).

4 Discussion

4.1 Foliar deposits analysis (quantity, size distribution and elemental composition)

The foliar deposits measured on oriental plane trees in this study (0.33 mg cm^{-2}) are very close to the findings of Heshmatol Vaezin et al. (2021), who measured foliar deposits along

Content courtesy of Springer Nature, terms of use apply. Rights reserved.

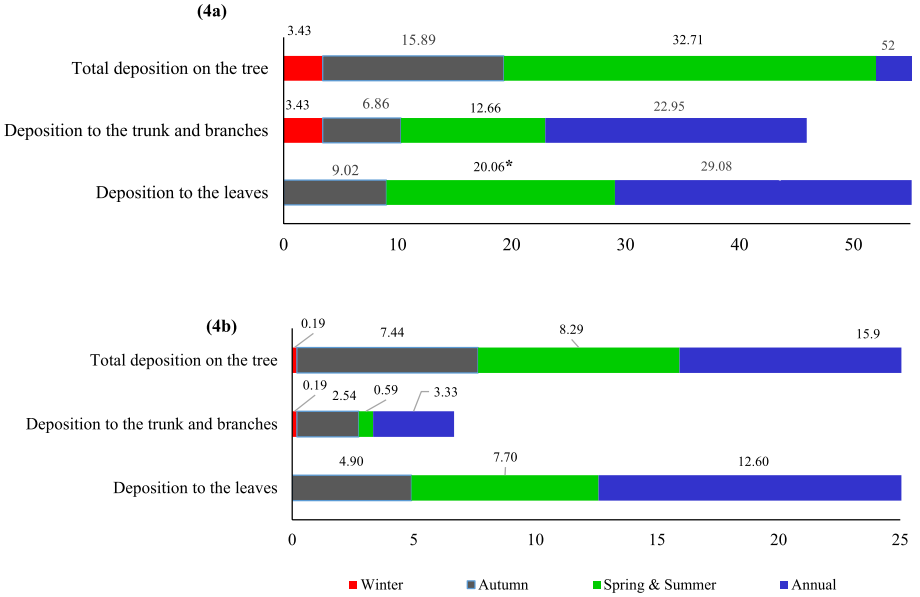


Fig. 6 PM_{10} deposition (g) on whole tree of oriental plane (6a) and white mulberry (6b) in Laleh Park in different season

Table 4 The average relative reduction (%) of PM_{10} by the park trees studied across diffrent scales

Period	Oriental plane				White mulberry			
	Laleh Park		6th district		Laleh Park		6th district	
	Respiratory height (m)	Boundary layer (m)	Respiratory height (m)	Boundary layer (m)	Respiratory height (m)	Boundary layer (m)	Respiratory height (m)	Boundary layer (m)
Spring–summer	13.6	0.04	7.1	0.02	1.0	0.0	3.9	0.0
Autumn	8.0	0.03	6.2	0.02	0.6	0.0	1.9	0.0
Winter	1.9	0.01	1.3	0.00	0.0	0.0	0.0	0.0
Annual	9.3	0.03	5.4	0.02	0.7	0.0	2.4	0.0

Valiasr Street in Tehran (0.34 mg cm^{-2}). Similarly, these results are comparable to those of Elkaee Behjati (2019), who measured foliar deposits of 0.43 mg cm^{-2} on oriental plane leaves along Gandhi Street in Tehran. The discrepancy between these results may be partially attributed to differences in ambient PM_{10} concentrations, which directly influence PM_{10} deposition (Li et al., 2019; Perini et al., 2017; Setälä et al., 2013). This explains why the downwind gradients of ambient PM_{10} concentrations and foliar PM_{10} deposition in Laleh Park (Fig. 5) exhibited a nearly identical trend and slope.

Content courtesy of Springer Nature, terms of use apply. Rights reserved.

The mass of PM_{10} deposited on tree leaves was determined using the weight percentage of PM_{10} in the foliar deposits. Generally, a weight percentage of PM_{10} in foliar deposits around 50% is considered realistic, as close to 50% of TSP in urban air consists of PM_{10} (WHO, 2019). This confirms a proportional relationship between the weight percentage of PM_{10} in TSP and that in foliar deposits. Nevertheless, difference between tree species—particularly in leaf surface roughness (due to features like cuticle and trichromes) and tree morphology including crown and foliage size and structure—may explain variations in the weight percentage of PM_{10} in foliar deposits, especially for smaller particles (Beckett et al., 1998; Li et al., 2019; Sgrigna et al., 2015).

Most studies on the elemental composition of foliar deposits report a similar list such as Zn, Mn, Cu, Pb, Cr, Ce, Ni, Co, Al, and Fe, though the order of concentrations typically varies (Castanheiro et al., 2016; Molnár et al., 2020; Sawidis et al., 2011; Vercauteren et al., 2011). For instance, Rezayani et al. (2022) obtained an almost identical order of elemental composition (Zn, Cu, Pb, Cr, and Ni) in terms of concentrations in the same region. Moreover, the elemental composition of foliar deposits in this study showed extremely high and significant enrichment of Al and Pb, originating from both geogenic (Wang et al., 2007; Farzadkia et al., 2024) and anthropogenic (traffic–related) sources (Wang et al., 2007; Krupnova et al., 2020; Rezayani et al., 2022; Mostafa et al., 2024). Also, Aluminum, an important element in the Earth's crust, is used with the AL/Zn ratio to identify sources of TSP pollution. The Al/Zn = 0.001 ratio in this study, indicates significant vehicular emissions (Na & Cocker, 2009).

4.2 Deposition velocity

Deposition velocity is a key factor in the deposition flux model (Freer-Smith et al., 2005). For this reason, the average foliar deposition velocity for PM_{10} and $PM_{2.5}$ were estimated locally during the spring–summer period. However, finding comparable results in the literature is challenging, as deposition velocity is influenced by various factors, including species properties (e.g., LAI), planting schemes (Beckett et al., 1998), particle size (gravity), PM_{10} concentration (Sohrab et al., 2022), and wind speed (Pröhl et al., 2012). Nonetheless, the average deposition velocity for $PM_{2.5}$ on oriental plane trees at the study site, with a wind speed of 1.5 m s^{-1} (0.0011 m s^{-1}), falls within the rage of values (0.0003–0.0013 m s^{-1}) measured for different hardwood trees exposed to $PM_{2.5}$-like particles (mean diameter 1.28 μm) at a wind speed of 1 m s^{-1}, as reported by Beckett et al. (2000) through an experimental wind tunnel method. Moreover, the estimated deposition velocity for PM_{10} (0.0017 m s^{-1}) on oriental plane trees with a LAI of 2.2 (m^2 m^{-2}) at the study site is consistent with the reported value of 0.0064 m s^{-1} for a LAI of 6 (m^2 m^{-2}; Escobedo & Nowak, 2009; Hirabayashi, 2014; Pace, 2019). As expected, due to gravitational settling, we found a higher deposition velocity for PM_{10} (0.0017 m s^{-1}) compared to $PM_{2.5}$ (0.0011 m s^{-1}), which aligns with findings in the literature (Xing & Brimblecombe, 2019).

4.3 Relative reduction effect

Empirical evidence from direct measurements of ambient PM_{10} showed that the park's vegetation (trees and shrubs) reduced ambient PM_{10} at the respiratory level inside the park by an vaerage of 10.4% throughout the year. This result was strongly supported by indirect measurements on park trees (Table 4). Together, these findings are consistent with the air quality improvement rates reported in the literature, which ranges from 0.2% to 26% (Heshmatol Vaezin et al., 2021; Vigevani et al., 2024; Xing & Brimblecombe, 2019). Overall, we observed

Content courtesy of Springer Nature, terms of use apply. Rights reserved.

an average relative reduction of 16.5% in ambient PM_{10} at the respiratory level inside the park through a combination of deposition on vegetation (10.4%) and the dispersion of particles (6.1%). The downwind gradient of foliar PM_{10} deposition—obtained through indirect measurements of PM_{10} (Fig. 5)—further supports this combined effect, showing an average relative reduction of 16.5% inside the park. This reinforces the relevance of both direct and indirect measurements of PM_{10} in evaluating the effectiveness of urban parks in reducing ambient PM_{10} levels. Consistently, this finding is comparable to Yin et al. (2011), who estimated that urban parks in Shanghai (China), may reduce TSP by up to 35%, corresponding to approximately 17.5% in terms of PM_{10}.

5 Conclusion

The average relative reduction effect of urban parks on PM_{10} can be remarkable (16.5%), as it combines the impact of park trees through dry deposition (10.4%) and PM_{10} dispersion (6.1%) inside the park (Yin et al., 2011). Nevertheless, larger parks with greater depth may enhance the average reduction effect inside the park, as dispersion increases over a longer pollution diffusion distance from the pollutant source (e.g. urban traffic). By contrats, the confinement of pollution sources by dense park's trees may contribute to higher concentration of PM_{10} near the park, potentially affecting the PM_{10} gradient and reducing the average reduction effect inside the park. These findings underscore the vital role of well-designed urban parks in mitigating air pollution, highlighting the need for strategic urban planning to maximize their effectiveness in improving air quality. Further research is needed to assess the broader effectiveness of various types of urban green spaces (e.g., urban forests, parks, community gardens, and greenways) and plant species in mitigating different types of pollutants.

The combined empirical and theoretical procedure (Fig. 1) in this study offers a practical approach for urban planners and environmental policymakers, providing a framework to evaluate the average relative reduction of PM_{10} in urban parks. Such assessments allows for the selection of tree species and park designs that maximize air quality benefits, especially in pollution-prone urban settings. Our findings advocate for further research into the multifaceted role of urban parks in air pollution mitigation, particularly in terms of how park design and vegetation structure affect air quality across various urban contexts. Expanding this research to include different pollutant types (e.g., SO_2, NO_2, and O_3), urban configurations (e.g., urban canyons), and vegetation characteristics (e.g., vertical layering) will deepen our understanding of how green spaces can be strategically designed to enhance urban greening and public health.

Appendix A

The canopy cover area (CCA; m^2), total leaf area (TLA; m^2), and leaf number (N) for each tree were estimated using following equations:

$$CCA = \left(\frac{D_1 \times D_2}{4}\right) \times \pi \tag{8}$$

Content courtesy of Springer Nature, terms of use apply. Rights reserved.

$$TLA = LAI \times CCA \tag{9}$$

$$N = \frac{TLA}{ALA} \tag{10}$$

where D_1 and D_2 represent the large and small diameters of the tree crown (m). N is the number of leaves per tree in the study site during summer, and ALA (m^2) denotes the average leaf area of individual trees. ALA was estimated based on the average leaf area of sample leaves measured using ImageJ software (Ver. 1.52a).

Appendix B (Adapted from Heshmatol Vaezin et al., 2021)

We determined the dry deposition velocity of PM_{10} using the methodology outlined by Freer-Smith et al. (2005), expressed as:

$$VD_{1,2} = \frac{F_{1,2}}{C(H)_{1,2}} \tag{11}$$

where $VD_{1,2}$ denotes the species-specific dry deposition velocity during seasons 1 and 2 (e.g., spring and summer), $F_{1,2}$ represents the instantaneous deposition flux per unit leaf area ($\mu g\ m^{-2}\ s^{-1}$), and $C(H)_{1,2}$ is the local PM_{10} concentration at respiratory height (H) during spring and summer. Then, we estimate the dry deposition velocity in autumn and winter based on seasonal changes in LAI, following the method outlined by Hirabayashi (2014) as follows:

$$VD_i = VD_{1,2} \times \frac{BAI + LAI_i}{PAI_{1,2}} \tag{12}$$

where VD_i ($m\ s^{-1}$) and $VD_{1,2}$ ($m\ s^{-1}$) represent the calculated dry deposition velocities for season *i* (e.g., autumn or winter) and for spring and summer, respectively. BAI is the bark area index ($m^2\ m^{-2}$), LAI_i is the seasonal leaf area index in season *i*, and $PAI_{1,2}$ denotes the plant area index for spring and summer.

Acknowledgements The authors would like to acknowledge the Department of Forestry and Forest Economics at the University of Tehran, the Green Space Research Unit of the 6th District Municipality Tehran, and the Geological Survey and Mineral Explorations of Iran for their support and contributions to this study. The corresponding author extends his gratitude to Eng. Arash Daei, who undoubtedly paved the way for this research with his brilliant Master's thesis.

Author contribution MMJ Conceptualization, Data curation, Formal analysis, Software, Investigation, Methodology, Project administration, Resources, Writing—original draft, Writing—review and editing. SMHV Conceptualization, Data curation, Formal analysis, Software, Investigation, Methodology, Supervision, Writing—review and editing. MM Conceptualization, Funding acquisition, Data curation, Supervision. SH Conceptualization, Writing—review and editing. AS Supervision. RS Data curation, Funding acquisition. NA Data curation, Formal analysis. SMMS Software, Writing—original draft, Supervision, Writing—review and editing.

Data availability Data generated or analyzed during this study are available upon request from the corresponding author, with no restrictions.

Content courtesy of Springer Nature, terms of use apply. Rights reserved.

References

Abbaspour, M., Javid, A. H., & Saeidi, S. (2014). The impact of urban parks on PM_{10} suspended particles, through using GIS software. *Journal of Environmental Science and Technology*, *16*(1), 1–11.

Baldacchini, C., Castanheiro, A., Maghakyan, N., Sgrigna, G., Verhelst, J., Alonso, R., Amorim, J. H., Bellan, P., Bojović, D. Đ., Breuste, J., & Buhler, O. (2017). How does the amount and composition of PM deposited on Platanus acerifolia leaves change across different cities in Europe?. *Environmental science & Technology*, *51*(3), 1147–1156.

Beckett, K. P., Freer-smith, P. H., & Taylor, G. (1998). Urban woodlands: Their role in reducing the effects of particulate pollution. *Environmental Pollution*, *99*, 347–360. https://doi.org/10.1016/S0269-7491(98)00016-5

Beckett, K. P., Freer Smith, P. H., & Taylor, G. (2000). Effective tree species for local air quality management. *Arboricultural Journal*, *26*(1), 12–19.

Blanco, F. F., & Folegatti, M. V. (2003). A new method for estimating the leaf area index of cucumber and tomato plants. *Horticultura Brasileira*, *21*(4), 666–669. https://doi.org/10.1590/S0102-05362003000400019

Castanheiro, A., Samson, R., & De Wael, K. (2016). Magnetic- and particle-based techniques to investigate metal deposition on urban green. *Science of the Total Environment*, *571*(2016), 594–602. https://doi.org/10.1016/j.scitotenv.2016.07.026

Chamberlain, A. C. (1953). Aspects of travel and deposition of aerosol and vapor clouds. AERE HP/R 1261. Atomic Energy Research Establishment, Harwell, England.

Cochran. (2012). Determination of Appropriate Sample Size. In *International Journal of Applied Mathematics and Statistical Sciences* (Vol. 2). Bulletin of the Gauhati University Mathematics Association. https://doi.org/10.1016/j.ijpe.2004.09.004

Dadey, K. A., Janecek, T., & Klaus, A. (1992). Dry-bulk density: Its use and determination. *Proc., Scientific Results, ODP, Leg 126. Bonin Arc/trench System*, *126*, 551–554. https://doi.org/10.2973/odp.proc.sr.126.157.1992

Deljouei, A., Sadeghi, S. M. M., Abdi, E., Bernhardt-Römermann, M., Pascoe, E. L., & Marcantonio, M. (2018). The impact of road disturbance on vegetation and soil properties in a beech stand, Hyrcanian forest. *European Journal of Forest Research*, *137*(6), 759–770. https://doi.org/10.1007/s10342-018-1138-8

Elkaee Behjati, S. (2019). A relative analysis of carbon and dust uptake by important tree species in Tehran Iran. *International Journal of Environmental and Ecological Engineering*, *13*, 222–225.

Escobedo, F. J., & Nowak, D. J. (2009). Spatial heterogeneity and air pollution removal by an urban forest. *Landscape and Urban Planning*, *90*(3–4), 102–110. https://doi.org/10.1016/j.landurbplan.2008.10.021

Escobedo, F. J., Wagner, J. E., Nowak, D. J., la Maza, C. L., Rodriguez, M., & Crane, D. E. (2008). Analyzing the cost effectiveness of Santiago, Chile's policy of using urban forests to improve air quality. *Journal of Environmental Management*, *86*(1), 148–157. https://doi.org/10.1016/j.jenvman.2006.11.029

Farzadkia, M., Yavary Nia, M., Yavari Nia, M., Shacheri, F., Nourali, Z., & Torkashvand, J. (2024). Reduction of the environmental and health consequences of cigarette butt recycling by removal of toxic and carcinogenic compounds from its leachate. *Environmental Science and Pollution Research*, *31*(16), 23942–23950. https://doi.org/10.1007/s11356-024-32703-5

Freer-Smith, P. H., Beckett, K. P., & Taylor, G. (2005). Deposition velocities to *Sorbus aria*, *Acer campestre*, *Populus deltoides* × *trichocarpa* 'Beaupre, *Pinus nigra* and × *Cupressocyparis leylandii* for coarse, fine and ultra-fine particles in the urban environment. *Environmental Pollution*, *133*, 157–167.

Heist, D., Isakov, V., Perry, S., Snyder, M., Venkatram, A., Hood, C., Stocker, J., Carruthers, D., Arunachalam, S., & Owen, R. C. (2013). Estimating near-road pollutant dispersion: A model intercomparison. *Transportation Research Part D: Transport and Environment*, *25*, 93–105. https://doi.org/10.1016/j.trd.2013.09.003

Heshmatol Vaezin, S. M., Juybari, M. M., Daei, A., Avatefi Hemmat, M., Shirvany, A., Tallis, M. J., Hirabayashi, S., Moeinaddini, M., Hamidian, A. H., Sadeghi, S. M. M., & Pypker, T. G. (2021). The effectiveness of urban trees in reducing airborne particulate matter by dry deposition in Tehran. *Iran. Environmental Monitoring and Assessment*, *193*, 842. https://doi.org/10.1007/s10661-021-09616-8

Hirabayashi, S. (2014). i-Tree canopy air pollutant removal and monetary value model descriptions. 2010, 1–11. https://drive.google.com/open?id=0B2HZtylBeVjXT21FdDFaZzFITTQ

Hirabayashi, S., Kroll, C. N., & Nowak, D. J. (2012). Development of a distributed air pollutant dry deposition modeling framework. *Environmental Pollution*, *171*, 9–17. https://doi.org/10.1016/j.envpol.2012.07.002

Content courtesy of Springer Nature, terms of use apply. Rights reserved.

Janhäll, S. (2015). Review on urban vegetation and particle air pollution—Deposition and dispersion. *Atmospheric Environment*, *105*, 130–137. https://doi.org/10.1016/j.atmosenv.2015.01.052

Krupnova, T. G., Rakova, O. V., Gavrilkina, S. V., Antoshkina, E. G., Baranov, E. O., & Yakimova, O. N. (2020). Road dust trace elements contamination, sources, dispersed composition, and human health risk in Chelyabinsk, Russia. *Chemosphere*, *261*, 127799. https://doi.org/10.1016/j.chemosphere.2020.127799

Li, C., Huang, Y., Guo, H., Wu, G., Wang, Y., Li, W., & Cui, L. (2019). The concentrations and removal effects of PM_{10} and $PM_{2.5}$ on a Wetland in Beijing. *Sustainability*, *11*(5), 1–15. https://doi.org/10.3390/su11051312

Lovett, G. M. (1994). Atmospheric deposition of nutrients and pollutants in North America: an ecological perspective. *Ecological Applications*, *4*(4), 629-650.

Memoli, V., Esposito, F., Santorufo, L., Panico, S. C., Trifuoggi, M., Di Natale, G., & Maisto, G. (2020). Relationships between leaf exposure time to air pollution and metal and particulate matter accumulation for holm oak leaves. *Water, Air, and Soil Pollution*, *231*, 529. https://doi.org/10.1007/s11270-020-04894-3

Mihankhah, T., Saeedi, M., & Karbassi, A. (2020). A comparative study of elemental pollution and health risk assessment in urban dust of different land-uses in Tehran's urban area. *Chemosphere*, *241*, 124984.

Molnár, V. É., Tőzsér, D., Szabó, S., Tóthmérész, B., & Simon, E. (2020). Use of leaves as bioindicator to assess air pollution based on composite proxy measure (Apti), dust amount and elemental concentration of metals. *Plants*, *9*(12), 1–11. https://doi.org/10.3390/plants9121743

Morakinyo, T. E., & Lam, Y. F. (2016). Study of traffic-related pollutant removal from street canyon with trees: Dispersion and deposition perspective. *Environmental Science and Pollution Research*, *23*(21), 21652–21668. https://doi.org/10.1007/s11356-016-7322-9

Mostafa, M. T., El-Nady, H., Gomaa, R. M., Abdelgawad, H. F., Abdelhafiz, M. A., Salman, S. A. E., & Khalifa, I. H. (2024). Urban geochemistry of heavy metals in road dust from Cairo megacity, Egypt: Enrichment, sources, contamination, and health risks. *Environmental Earth Sciences*, *83*(1), 37. https://doi.org/10.1007/s12665-023-11342-y

Municipality of Tehran. (2023). *Tehran's Green Space Master Plan* (pp. 1–200). Tehran Urban Research and Planning Center: Tehran, Iran.

Na, K., & Cocker, D. R. (2009). Characterization and source identification of trace elements in $PM_{2.5}$ from Mira Loma, Southern California. *Atmospheric Research*, *93*(4), 793–800. https://doi.org/10.1016/j.atmosres.2009.03.012

Nowak, D. J. D., & Crane, D. D. E. (1998). The urban forest effects (UFORE) model: Quantifying urban forest structure and function. *Integrated Tools Proceedings*, *212*, 714–720. https://doi.org/10.3109/14017437509138634

Nowak, D. J., Crane, D. E., & Stevens, J. C. (2006). Air pollution removal by urban trees and shrubs in the United States. *Urban Forestry & Urban Greening, 4*(3–4), 115–123. https://doi.org/10.1016/j.ufug.2006.01.007

Nowak, D. J., Hirabayashi, S., Bodine, A., & Greenfield, E. (2014). Tree and forest effects on air quality and human health in the United States. *Environmental Pollution*, *193*, 119–129. https://doi.org/10.1016/j.envpol.2014.05.028

Pace, R. (2019). Modeling ecosystem services for park trees: Sensitivity of i-tree eco simulations to light exposure and tree species classification. *Forests*, *9*, 1–18. https://doi.org/10.3390/f9020089

Perini, K., Ottelé, M., Giulini, S., Magliocco, A., & Roccotiello, E. (2017). Quantification of fine dust deposition on different plant species in a vertical greening system. *Ecological Engineering*, *100*, 268–276. https://doi.org/10.1016/j.ecoleng.2016.12.032

Pröhl, G., Twining, J. R., & Crawford, J. (2012). Radiological consequences modelling. *Radioactivity in the Environment*, *18*, 281–342.

Rasoolzadeh, R., Mobarghaee Dinan, N., Esmaeilzadeh, H., Rashidi, Y., Marcu, M. V., & Sadeghi, S. M. M. (2024a). Carbon sequestration and storage of urban trees in a polluted semiarid city. *Forests*, *15*(9), 1488. https://doi.org/10.3390/f15091488

Rasoolzadeh, R., Mobarghaee Dinan, N., Esmaeilzadeh, H., Rashidi, Y., Marcu, M. V., & Sadeghi, S. M. M. (2024b). *Assessment of air pollution removal by urban trees based on the i-Tree eco model: The case of Tehran*. Integrated Environmental Assessment and Management.

Rezayani, N., Mirmohammadi, M., & Mehrdadi, N. (2022). Origin and risk assessment, and evaluation of heavy metal pollution in the soil and air of Tehran (case study: central district in Tehran city). *International Journal of Environmental Science and Technology*, *19*(8), 7337–7358.

Sadeghi, S. M. M., Van Stan, J. T., Pypker, T. G., & Friesen, J. (2017). Canopy hydrometeorological dynamics across a chronosequence of a globally invasive species, *Ailanthus altissima* (Mill., tree of heaven). *Agricultural and Forest Meteorology, 240*, 10–17. https://doi.org/10.1016/j.agrformet.2017.03.017

Content courtesy of Springer Nature, terms of use apply. Rights reserved.

Sakunkoo, P., Thonglua, T., Sangkham, S., Jirapornkul, C., Limmongkon, Y., Daduang, S., Tessiri, T., Rayubkul, J., Thongtip, S., Maneenin, N., & Pimonsree, S. (2022). Human health risk assessment of $PM_{2.5}$-bound heavy metal of anthropogenic sources in the Khon Kaen Province of Northeast Thailand. *Heliyon*, *8*(6), e09572. https://doi.org/10.1016/j.heliyon.2022.e09572

Sawidis, T., Breuste, J., Mitrovic, M., Pavlovic, P., & Tsigaridas, K. (2011). Trees as bioindicator of heavy metal pollution in three European cities. *Environmental Pollution*, *159*(12), 3560–3570. https://doi.org/10.1016/j.envpol.2011.08.008

Setälä, H., Viippola, V., Rantalainen, A., Pennanen, A., & Yli-pelkonen, V. (2013). Does urban vegetation mitigate air pollution in northern conditions? *Environmental Pollution*, *183*, 104–112. https://doi.org/10.1016/j.envpol.2012.11.010

Sgrigna, G., Sæbø, A., Gawronski, S., Popek, R., & Calfapietra, C. (2015). Particulate Matter deposition on *Quercus ilex* leaves in an industrial city of central Italy. *Environmental Pollution*, *197*, 187–194. https://doi.org/10.1016/j.envpol.2014.11.030

Sohrab, S., Csikós, N., & Szilassi, P. (2022). Connection between the spatial characteristics of the road and railway networks and the air pollution (PM10) in urban–rural fringe zones. *Sustainability*, *14*(16), 10103.

Song, Y., Maher, B. A., Li, F., Wang, X., Sun, X., & Zhang, H. (2015a). Particulate matter deposited on leaf of five evergreen species in Beijing, China: Source identification and size distribution. *Atmospheric Environment*, *105*, 53–60. https://doi.org/10.1016/j.atmosenv.2015.01.032

Tallis, M. J., Taylor, G., Sinnett, D., & Freer-Smith, P. (2011). Estimating the removal of atmospheric particulate pollution by the urban tree canopy of London, under current and future environments. *Landscape and Urban Planning*, *103*(2), 129–138. https://doi.org/10.1016/j.landurbplan.2011.07.003

Vercauteren, J., Matheeussen, C., Wauters, E., Roekens, E., Grieken, R. V., Krata, A., Makarovska, Y., Maenhaut, W., Chi, X., & Geypens, B. (2011). Chemkar PM10: An extensive look at the local differences in chemical composition of PM_{10} in Flanders, Belgium. *Atmospheric Environment*, *45*(1), 108–116. https://doi.org/10.1016/j.atmosenv.2010.09.040

Vigevani, I., Corsini, D., Comin, S., Fini, A., & Ferrini, F. (2024). Methods to quantify particle air pollution removal by urban vegetation: a review. *Atmospheric Environment: X*, *21*, 100233. https://doi.org/10.1016/j.aeaoa.2023.100233

Wang, L., Hasi, E., Liu, L. Y., & Gao, S. Y. (2007). Physico-chemical characteristics of ambient particles settling upon leaf surface of six conifers in Beijing. *Ying Yong Sheng tai xue bao= The Journal of Applied Ecology*, *18*(3), 487–492.

WHO. (2019). *Ambient (Outdoor) Air Quality and Health*. Available online: https://www.who.int/news-room/factsheets/detail/ambient-(outdoor)-air-quality-and-health. Accessed on 12 January 2023.

WHO. (2021). WHO global air quality guidelines: Particulate matter ($PM_{2.5}$ and PM_{10}), ozone, nitrogen dioxide, sulfurdioxide and carbon monoxide. World Health Organization. Available at: https://www.who.int/publications/i/item/9789240034228

Xing, Y., & Brimblecombe, P. (2019). Role of vegetation in deposition and dispersion of air pollution in urban parks. *Atmospheric Environment*, *201*, 73–83.

Yin, S., Shen, Z., Zhou, P., Zou, X., Che, S., & Wang, W. (2011). Quantifying air pollution attenuation within urban parks: An experimental approach in Shanghai, China. *Environmental pollution*, *159*(8–9), 2155–2163.

Zoller, W. H., Gladney, E. S., & Duce, R. A. (1974). Atmospheric concentrations and sources of trace metals at the South Pole. *Science*, *183*(4121), 198–200. https://doi.org/10.1126/science.183.4121.198

Publisher's Note Springer Nature remains neutral with regard to jurisdictional claims in published maps and institutional affiliations.

Springer Nature or its licensor (e.g. a society or other partner) holds exclusive rights to this article under a publishing agreement with the author(s) or other rightsholder(s); author self-archiving of the accepted manuscript version of this article is solely governed by the terms of such publishing agreement and applicable law.

Content courtesy of Springer Nature, terms of use apply. Rights reserved.

Authors and Affiliations

Mohammad Moftakhar Juybari[1] · Seyed Mahdi Heshmatol Vaezin[1] · Mazaher Moeinaddini[5] · Satoshi Hirabayashi[2] · Anoshirvan Shirvany[1] · Reza Shahbazi[3] · Nahid Ahmadi[3] · Seyed Mohammad Moein Sadeghi[4]

✉ Seyed Mahdi Heshmatol Vaezin
mheshmat@ut.ac.ir

[1] Department of Forestry and Forest Economics, University College of Agriculture and Natural Resources, University of Tehran, Karaj 77871-31587, Islamic Republic of Iran

[2] The Davey Tree Expert Company, Kent, OH 44240, USA

[3] Geological Survey of Iran, Tehran, Islamic Republic of Iran

[4] School of Forest, Fisheries, and Geomatics Sciences, University of Florida, Gainesville, FL, USA

[5] Department of Environmental Sciences, University of Tehran, Karaj, Iran

Content courtesy of Springer Nature, terms of use apply. Rights reserved.

Terms and Conditions

Springer Nature journal content, brought to you courtesy of Springer Nature Customer Service Center GmbH ("Springer Nature").

Springer Nature supports a reasonable amount of sharing of research papers by authors, subscribers and authorised users ("Users"), for small-scale personal, non-commercial use provided that all copyright, trade and service marks and other proprietary notices are maintained. By accessing, sharing, receiving or otherwise using the Springer Nature journal content you agree to these terms of use ("Terms"). For these purposes, Springer Nature considers academic use (by researchers and students) to be non-commercial.

These Terms are supplementary and will apply in addition to any applicable website terms and conditions, a relevant site licence or a personal subscription. These Terms will prevail over any conflict or ambiguity with regards to the relevant terms, a site licence or a personal subscription (to the extent of the conflict or ambiguity only). For Creative Commons-licensed articles, the terms of the Creative Commons license used will apply.

We collect and use personal data to provide access to the Springer Nature journal content. We may also use these personal data internally within ResearchGate and Springer Nature and as agreed share it, in an anonymised way, for purposes of tracking, analysis and reporting. We will not otherwise disclose your personal data outside the ResearchGate or the Springer Nature group of companies unless we have your permission as detailed in the Privacy Policy.

While Users may use the Springer Nature journal content for small scale, personal non-commercial use, it is important to note that Users may not:

1. use such content for the purpose of providing other users with access on a regular or large scale basis or as a means to circumvent access control;
2. use such content where to do so would be considered a criminal or statutory offence in any jurisdiction, or gives rise to civil liability, or is otherwise unlawful;
3. falsely or misleadingly imply or suggest endorsement, approval , sponsorship, or association unless explicitly agreed to by Springer Nature in writing;
4. use bots or other automated methods to access the content or redirect messages
5. override any security feature or exclusionary protocol; or
6. share the content in order to create substitute for Springer Nature products or services or a systematic database of Springer Nature journal content.

In line with the restriction against commercial use, Springer Nature does not permit the creation of a product or service that creates revenue, royalties, rent or income from our content or its inclusion as part of a paid for service or for other commercial gain. Springer Nature journal content cannot be used for inter-library loans and librarians may not upload Springer Nature journal content on a large scale into their, or any other, institutional repository.

These terms of use are reviewed regularly and may be amended at any time. Springer Nature is not obligated to publish any information or content on this website and may remove it or features or functionality at our sole discretion, at any time with or without notice. Springer Nature may revoke this licence to you at any time and remove access to any copies of the Springer Nature journal content which have been saved.

To the fullest extent permitted by law, Springer Nature makes no warranties, representations or guarantees to Users, either express or implied with respect to the Springer nature journal content and all parties disclaim and waive any implied warranties or warranties imposed by law, including merchantability or fitness for any particular purpose.

Please note that these rights do not automatically extend to content, data or other material published by Springer Nature that may be licensed from third parties.

If you would like to use or distribute our Springer Nature journal content to a wider audience or on a regular basis or in any other manner not expressly permitted by these Terms, please contact Springer Nature at

onlineservice@springernature.com